JOURNAL OF OPTOELECTRONICS AND ADVANCED MATERIALS Vol. 9, No. 8, August 2007 p. 2529 - 2534

Enzymatic control of the bio-inspired nanomaterials at the spectroscopic level

M. V. PUTZ*, A.-M. LACRĂMĂ[a]
Laboratory of Computational and Structural Physical Chemistry, Chemistry Department, West University of Timişoara, Str. Pestalozzi No. 16, Timişoara, RO-300115, Romania
[a]*Laboratory of Biochemistry, Chemistry Department, West University of Timişoara, Str. Pestalozzi No. 16, Timişoara, RO-300115, Romania*

Aiming to improve the control of the biological regulation the fit of the enzymatic kinetics with the absorption spectrometry is unfolded in the frame of Michaelis-Menten mechanisms including inhibitions. In this context, the time-dependent expression of binding substrate concentration is considered through its *W*-Lambert form. Then, employing the authors' method of logistical transformations the progress curves of substrate and product reactants are revealed under their analytical expressions from where the specific effective reaction time is extracted as a measure of the ligand interactions. The presented method allows optimum choice of the spectroscopic method when marking biomaterials through the control of inhibited enzymes, depending on the output of the widths of substrate or product molecular absorption which indicate the fast-reaction ranges.

(Received November 15, 2006; accepted December 21, 2006)

Keywords: Enzymes, Michaelis-Menten kinetics, Inhibition, W-Lambert function, Beer-Lambert spectroscopy

1. Introduction

In current years the biomedical nanostructured systems have become highly researched due their impact on health and life insurance. Whatever the metal implants during osseointegration, human osteoblasts and macrophages, or dialysis membrane biocompatibility are studied, the tests regarding toxicity, long-term body responses and mutagenicity involve the controlling of the enzymes, e.g. metalloproteinases or the lactate dehydrogenase (LDH), as markers of cell damage through their interaction with the available bone and substrate [1-4]. The enormous promise of the enzyme biomarkers to detect the degree of biocompatibility of the implants and bio-inspired nanomaterials, targeting the clinical treatment of cancer as well the mutagenic diseases [5, 6], requires, among the cellular bioassays, the in-deep understanding and prediction of the enzymatic catalytic dynamical mechanism with and without inhibition, both in vitro and in vivo conditions.

The present work gives an analytically complete picture of the competitive, uncompetitive and mixed inhibition cases of the enzyme kinetics solving them for the temporal or dynamical concentration of reactants. Such endeavour provides the missing theoretical link between the consecrated rates of protein catalysis and the absorption spectroscopy through engaging the substrate progress curves to the effective times and energies of enzymatic reactions.

2. Theory

The starting point stands the paradigmatic Michaelis and Menten enzymic scheme of reaction [7, 8]:

$$E + S \underset{k_{-1}}{\overset{k_1}{\rightleftharpoons}} ES \xrightarrow{k_2} E + P \tag{1}$$

Equation (1) involves two stages of transformation of the substrate *S* into product *P* under the action of enzyme *E*: first one corresponds to the reversible formation of the enzyme-substrate *ES* with the microscopic rates k_1 and k_{-1}, while the second stage is dominated by the rate k_2 to irreversible release of the product molecule. Actually, we will treat the extended scheme of the mixed inhibition in which the basic reaction (1) is accompanied by the adjacent reversible competitive and uncompetitive reactions

$$E + I \underset{}{\overset{K_I}{\rightleftharpoons}} EI, \quad ES + I \underset{}{\overset{K_{IS}}{\rightleftharpoons}} ESI, \tag{2}$$

characterized by the macroscopic dissociation constants:

$$\mathrm{K_I} = \frac{[\mathrm{E}][\mathrm{I}]_0}{[\mathrm{EI}]}, \mathrm{K_{IS}} = \frac{[\mathrm{ES}][\mathrm{I}]_0}{[\mathrm{ESI}]}, \tag{3}$$

where $[I]_0$, $[E]$, $[ES]$, $[EI]$, $[ESI]$ represent concentrations of initial inhibitor, instantaneous enzyme as well as of enzyme-substrate, enzyme-inhibitor, and enzyme-substrate-inhibitor complexes, respectively.

In these conditions, the first problem is to find the overall reaction velocity $v = k_2[ES]$ expressed throughout the assumed parameters and by the current substrate concentration [*S*]. Then, one likes to further solve the obtained reaction velocity equation for the progress curves of the substrate or product concentrations.

To achieve the first goal the quasi steady state assumption (QSSA) of the *ES* complex is considered [9]:

$$\frac{d}{dt}[ES] \cong 0 \,. \tag{4}$$

Worth noting that the QSSA applies under common in vitro conditions in which the substrate is in great excess, usually over two orders, respecting enzyme [10]: $[S]_0 = \varepsilon^{-1}[E]_0$, $\varepsilon < 10^{-2}$. This way, the overall velocity of the coupled reactions (1) and (2) converts the substrate into the product according with [9]:'

$$v = \frac{d[P]}{dt} \equiv -\frac{d[S]}{dt} = \frac{V_{\max}[S]}{\alpha K_M + \alpha'[S]} \,. \tag{5}$$

In (5) the Michaelis constant defined $K_M = (k_{-1} + k_2)/k_1$ plays the role of the macroscopic dissociation constant of *ES* in reaction (1), while the introduced maximal velocity, $V_{\max} = k_2[E]_0$, occurs when the enzyme is saturated with substrate, i.e. when it is entirely in the *ES* form; the competitive and uncompetitive inhibition parameters were respectively introduced as:

$$\alpha = 1 + \frac{[I]_0}{K_I} \;,\; \alpha' = 1 + \frac{[I]_0}{K_{IS}} \tag{6}$$

The second theoretical goal is to solve the equation (5) for the substrate progress curve [*S*](*t*).

By formal integrating of equation (5) and through comparing the result with the famous *W*-Lambert function, defined through equation [11]:

$$W(x) + \ln W(x) = \ln(x) \;,\; x \geq -\exp(-1) \,, \tag{7}$$

the substrate time dependent concentration including inhibition comes out:

$$[S](t)^W = \frac{\alpha}{\alpha'} K_M W\left(\frac{\alpha'[E]_0}{\alpha \varepsilon K_M} \exp\left(\frac{\alpha'[E]_0}{\alpha \varepsilon K_M} \right) \exp\left(-\frac{t V_{\max}}{\alpha K_M} \right) \right), \tag{8}$$

when replaced also the initial substrate concentration with the enzyme one via its above ε - parametric relation.

The closed-form solution (8), originally proposed by Schnell and Mendoza in 1997 for the simple reaction (1), when $\alpha = \alpha' = 1$ [12], and then in 2001 to include also the effect of combined inhibitions (2) [13], is given in terms of a relatively unknown transcendental *W*-function. This clearly presents some limitations for its usability, because the implementation of this function is not widely available in fitting software when used to analyze the biological assay by means of enzymatic reactions. In next, the present work makes the advancement in proposing an analytical substitute for the intrinsic *W*-Lambert solution (8) still providing a better frame for fulfilling the quasi-steady-state approximation for enzyme catalysis.

3. Results

The stabilization mechanism of the transition state of the enzyme-substrate complex is realized by interaction of the substrate with the enzyme active site [14]. However, this hypothesis, still widely accepted due to experimental observation, is limited by what we can call "the enzymatic paradox". For instance, the reaction $E+S \rightarrow ES \rightarrow E+P$ represented by diagrammatically appropriate "lock and key" interactions looks like to be energetically forbidden. Such behaviour is due to the catalytic property of enzyme to be entirely recovered at the end of reaction. This picture is the analogue of the absorption-emission process in which the "photon role" is played by the enzyme: when the same amount of energy is released as achieved the excited state $|ES\rangle$ decays on the same initial state $|P\rangle \equiv |S\rangle$, see Fig. 1a. Searching for the solution of the enzymatic paradox the basic mechanism of the reaction (1) has to be substituted with the real enzymic reaction:

$$E + S \rightarrow ES \xrightarrow{\quad delay \quad} EP \rightarrow E + P \,. \tag{9}$$

Such mechanism agrees also with the *quasi*-steady-state condition of [*ES*], as prescribed by approximate equation (4), due to the intra-conversion of $|ES\rangle$ into $|EP\rangle$. Within this approach the enzymatic paradox is phenomenological solved, see Figure 1b.

On the other way, quantitatively, the working temporal substrate concentration dependence without inhibition ($\alpha = \alpha' = 1$) is shaped as:

$$[S](t)^W = K_M W\left(\frac{[E]_0}{\varepsilon K_M} \exp\left(\frac{[E]_0}{\varepsilon K_M} \right) \exp\left(-\frac{t V_{\max}}{K_M} \right) \right). \tag{10}$$

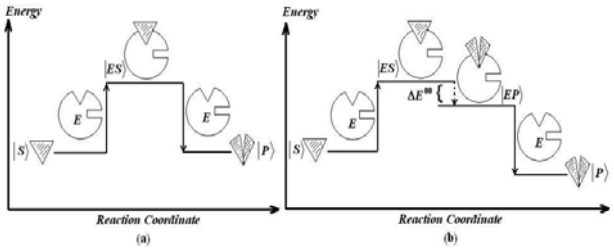

Fig. 1. (a) Energy level diagram of the enzyme-catalyzed reaction E+S→ES→E+P based on single intermediary ES complex. (b) Energy level diagram of the enzyme-catalyzed reaction E+S→ES→EP→E+P by means of two transition states, $|ES\rangle$ and $|EP\rangle$, separated by the energy of reaction ΔE^{00}. In both representations the reactants, enzyme (E), substrate (S), and product (P), and the intermediate molecular complexes (ES, EP) are depicted by their representative cartoons.

When bounded with the enzyme the substrate state transforms from $|ES\rangle$ to $|EP\rangle$ complex by suffering an internal (structural) perturbation. In analytical terms, this means that the solution (10) has to be slightly modified in such way that, preserving all the qualities of the enzymatic kinetic, to provide the required delay in product formation.

Such analytical passage was recently worked out [15], and assumes the general so called logistical transformation

$$f_1 W\left(f_2 \exp^{f_2} \exp^{-f_3 t}\right) \to f_1 \ln\left[1+\left(\exp^{f_2}-1\right)\exp^{-f_3 t}\right] \quad (11)$$

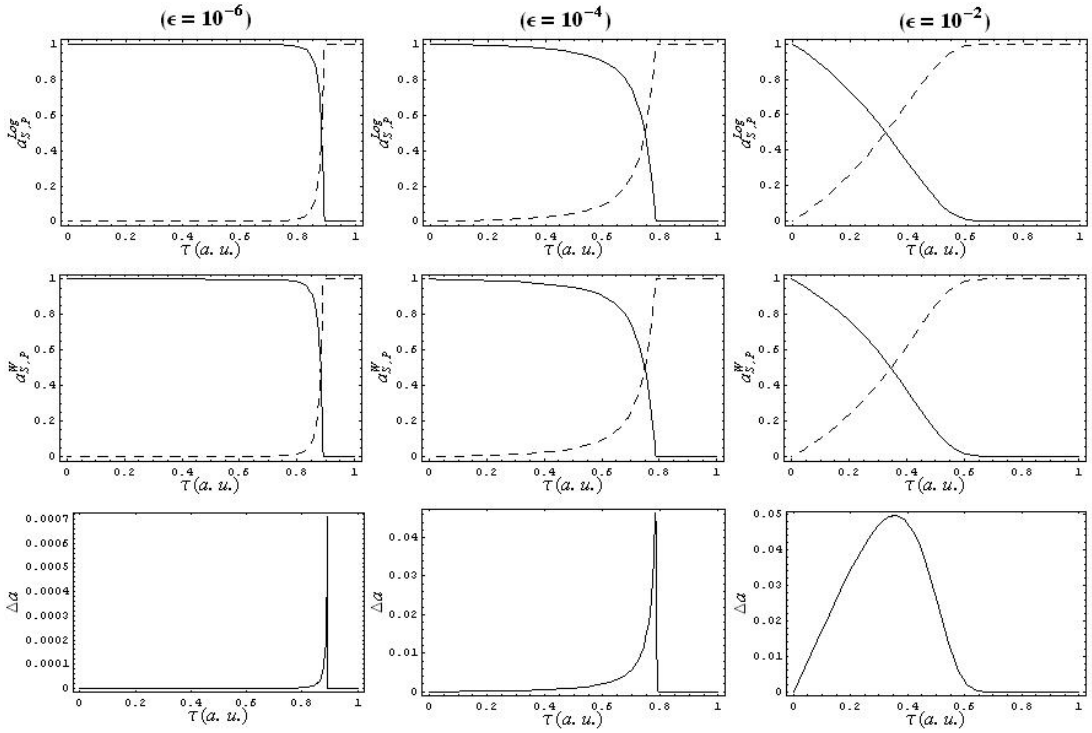

Fig. 2. *The first two rows show the normal absorptions for substrate (continuous curves) and product (dashed curves) concentrations of the enzyme-catalyzed reaction without inhibition, based on the logistical temporal approximation, and on the W-Lambert temporal solution, respectively; the third row depicts the difference between W-Lambert and logistical counterpart for substrate or product normal absorption progress curves; on columns there are presented the plots for the enzyme/substrate ratio ε taking the in vitro, from 10^{-6} to 10^{-4}, and almost the in vivo, equal of greater than 10^{-2}, values, respectively; the employed kinetic parameters are the maximum velocity of enzyme reaction $V_{\max}=10^{-4}M\cdot s^{-1}$ and the Michaelis constant $K_M=2\cdot 10^{-4}M$, while the total enzyme concentration is set at $[E]_0=10^{-6}M$; the time infinite range has been mapped onto the interval $(0,1)$ with the aid of the exponential time scale $\tau = 1-1/\ln(t+e)$ [12], being expressed in arbitrary units (a.u.).*

With (11) the respective logistical progress curve of the substrate solution (10) can be formulated:

$$[S](t)^{Log} = K_M \ln\left[1+\left(\exp\left(\frac{[E]_0}{\varepsilon K_M}\right)-1\right)\exp\left(-\frac{V_{\max}}{K_M}t\right)\right]. \quad (12)$$

Remarkably, the present substrate concentration progress curves, (10) and (12), can be used when measuring the enzymatic activity over substrate within absorption spectroscopy according to the adapted Beer-Lambert law [16]:

$$A_S(t) = a_M l[S](t). \quad (13)$$

However, considering the free substrate absorption $A_0 = a_M l[S]_0$, we can deal, for convenience, with the normal absorptivity of the substrate or of the product, respectively obtained:

$$a_S(t) = \frac{A_S(t)}{A_0} = \frac{[S](t)}{[S]_0},$$
$$a_P(t) = \frac{A_P(t)}{A_0} = \frac{[P](t)}{[S]_0} = 1 - a_S(t) - \frac{\varepsilon[S](t)}{[S](t)+K_M}, \quad (14)$$

since for the $a_P(t)$ expression the mass conservation laws of joint reactions (1) and (2), together with notations (3), have been used.

There came out that as the in vivo conditions are approached as the substrate is earlier catalyzed towards product with an extended time of reaction, see Fig. 2.

Searching for evidence of the real time of catalysis we have found that performing the normal absorption differences between intrinsic *W*-Lambert and the logistic representations of the substrate or product progress curves,

$$\Delta a(t) = a_S^W(t) - a_S^{Log}(t) \cong a_P^{Log}(t) - a_P^W(t), \quad (15)$$

one gets the absorption signal over the time interval of the enzymatic reaction, see the third row of Fig. 2.

There follows that the basic *W*-Lambert solution (10) closely characterizes the intrinsic $|ES\rangle$ state, while its perturbation expressed by the logistical form (12) is properly associated with the molecular complex $|EP\rangle$. Since we can define the effective time of reaction $\Delta\tau$ as the width at the half height of the recorded $\Delta a(t)$ signal, the energy ΔE^{00} of reaction (9) follows from the spectroscopic Heisenberg relation:

$$\Delta E \cong \frac{\hbar}{\Delta\tau}. \quad (16)$$

From the experimental point of view, the present algorithm prescribes the type of spectroscopy to be used, from pressure and temperature jumps until the electron paramagnetic resonance and electric field jumps, depending on the output of the effective times $\Delta\tau$ that fix the fast-reaction ranges [14], when assaying the enzymatic activity through absorption.

4. Discussion

The actual results can be extended also to the cases when different types and degrees of enzymatic inhibition are considered leading with important effects of biological regulations as will be in next exposed.

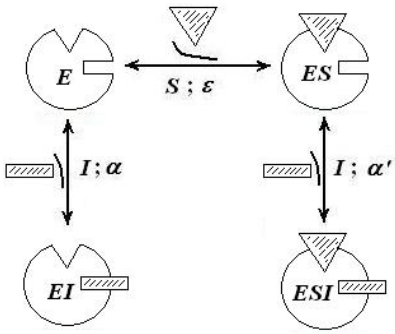

Fig. 3. Cartoon representation of the competitive and uncompetitive inhibitions acting through the inhibitor (I) on the enzyme (E) or on enzyme-substrate complex (ES), being quantified by α and α' parameters, respectively, for an enzyme-catalyzed reaction E+S→ES→EP→E+P.

The Fig. 3 depicts the main types of allosteric interactions involving enzymes. Note that the competitive inhibition, quantified by the parameter α of equation (6), appears when the inhibitor has an analogue molecular structure to that of substrate and binds with the enzyme on this complementarity ground. Typical examples are the anti-metabolites, e.g. the sulphanilamide as the competitive antagonist of the para-amino-benzoic acid (known as the H-vitamin), which blocking grows and multiplications of microorganisms have the bacterio-static effects. On the other way, when the inhibitor is acting upon the enzyme-substrate complex the uncompetitive inhibition type, quantified by the parameter α' of equation (6), regulates the enzymatic catalysis. This situation is specific to the in vivo occasions when, for instance, the adenosine three phosphatase inhibitor blocks the enzymes of glycol so controlling the energetic release in cell. However, the mixed inhibitions can also appear since both competitive and uncompetitive inhibitions take place in the course of complex biosynthesis [9].

The working substrate concentration will be now the basic *W*-Lambert solution (8) together with the respective logistical one,

$$[S]^{Log}(t) = \frac{\alpha}{\alpha'} K_M \ln\left[1 + \left(\exp\left(\frac{\alpha'[E]_0}{\alpha\varepsilon K_M}\right) - 1\right)\exp\left(-\frac{V_{\max}}{\alpha K_M}t\right)\right], \quad (17)$$

derived upon the transformation rule (11). With these, the difference for substrate or product normal absorptions (15) can be computed at different levels of inhibitions combined with various total enzyme/initial substrate ratios, see Fig. 4. By comparing the plots of the Fig. 4 with those corresponding to no inhibition case of Fig. 3 the hierarchy of the effective times of reactions yields:

$$\Delta\tau^{0\alpha'} < \Delta\tau^{\alpha\alpha'} < \Delta\tau^{00} < \Delta\tau^{\alpha 0},\ \varepsilon \in \left(10^{-6}, 10^{-4}\right), \quad (18)$$

$$\Delta\tau^{\alpha 0} < \Delta\tau^{\alpha\alpha'} < \Delta\tau^{00} < \Delta\tau^{0\alpha'},\ \varepsilon \geq 10^{-2}, \quad (19)$$

for the in vitro and in vivo environments, respectively.

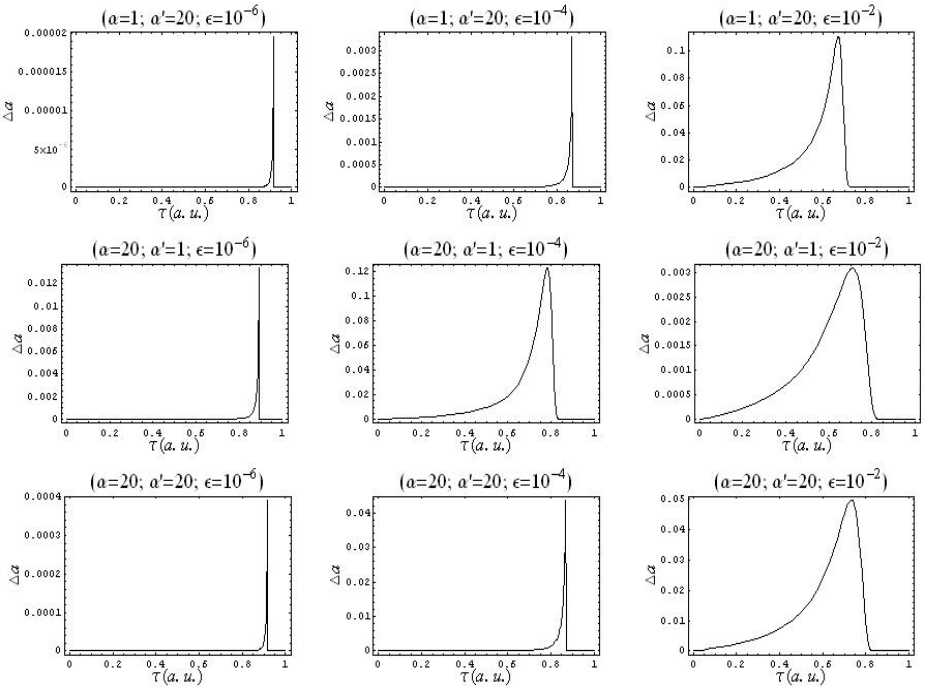

Fig. 4. Differences between W-Lambert and logistical counterparts for substrate or product normal absorption progress curves; on columns there are presented the plots for the enzyme/substrate ratio ε taking the in vitro, from 10^{-6} to 10^{-4}, and almost the in vivo, equal of greater than 10^{-2}, values, respectively; on rows different competitive and uncompetitive inhibition combinations quantified by the α and α' parameters, taking the values equal with 1 and 20, are respectively considered; the employed kinetic parameters and temporal scales are the same as used in Fig. 2.

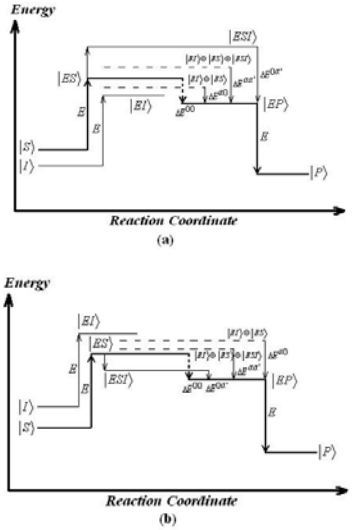

*Fig. 5. In vitro **(a)** and in vivo **(b)** energy level diagrams of the enzyme-catalyzed reaction E+S→ES→EP→E+P in the presence of the inhibitor (I) acting competitively on the enzyme (E), uncompetitively on enzyme-substrate complex (ES), or by mixed competition on both the enzyme and enzyme-substrate (the thin lines of mechanisms), in relation with the no inhibition case (the thick lined mechanism), providing the delayed time of specific reaction and the associated width of transition state energies, $\Delta E^{\alpha 0}$, $\Delta E^{0\alpha}$, $\Delta E^{\alpha\alpha'}$, and ΔE^{00}, respectively.*

Obviously, at the energetic level, due to the spectroscopic Heisenberg relation (16) the pecking orders of (18) and (19) reverse:

$$\Delta E^{0\alpha'} > \Delta E^{\alpha\alpha'} > \Delta E^{00} > \Delta E^{\alpha 0},\ \varepsilon \in \left(10^{-6}, 10^{-4}\right), \tag{20}$$

$$\Delta E^{\alpha 0} > \Delta E^{\alpha\alpha'} > \Delta E^{00} > \Delta E^{0\alpha'},\ \varepsilon \geq 10^{-2}. \tag{21}$$

These results can be phenomenological visualised from diagrams of Fig. 5 whose quantum mechanisms are based on next rules. First one recommends that the non inhibited transition state $|ES\rangle$ is always placed between inhibited intermediary complexes, $|EI\rangle$ and $|ESI\rangle$, as revealed from Fig. 3; then, the energy of inhibitor state $|I\rangle$ is higher in vivo than in vitro, respecting substrate $|S\rangle$, due to the crowding of the in vivo environment. Competitive inhibition is firstly considered, due to direct attack on enzyme; consequently, $|EI\rangle$ and $|ES\rangle$ are coexisting states and undergo quantum combination in a mixed new intermediary state $|EI\rangle \otimes |ES\rangle$; the uncompetitive inhibition state is the

quantum $|ESI\rangle$ state, being obtained from the state $|ES\rangle$ such that the first above rule to be obeyed; when both competitive $|EI\rangle \otimes |ES\rangle$ and uncompetitive $|ESI\rangle$ states are present they further combine and the new mixed intermediary quantum $|EI\rangle \otimes |ES\rangle \otimes |ESI\rangle$ state arises, which always has to lay above of $|ES\rangle$ one; all new inhibited intermediary states decay on the same $|EP\rangle$ state as in the case of no inhibition. It follows that the differences respecting the no inhibition case occur from the induced energetic width with which the inhibited transition states regulate the delayed times of catalysis. With these, the diagrams of Fig. 5 recover the analytical results (20) and (21).

5. Conclusions

The present venture was dedicated in questing for practical estimates of temporal scales when controlling the enzymatic activity with inhibition at the spectroscopic level. There comes out that it can be extended also in the line of elucidation of the quantum mechanism of the altered heritable gene expression from the product formation by delays in proteomic and complex enzymic interactions in cells. Applications of this approach include the marking of bio-inspired nanomaterials through assaying the enzymatic activity and the control of the metabolic processes and gene expressions by the natural or implanted inhibitors. The current view may as well contribute for future reconciliation of the reductionism with the wholism in biophysical medicine.

Acknowledgements

This work was carried out due to the generous support from Romanian National Council of Scientific Research in Universities (CNCSIS) by Grant AT/54/2006. A.-M.L. is indebt to Prof. Dr. Vasile Ostafe from Chemistry Department of West University of Timişoara for his kind in encouraging her on the line of theoretical enzymatic research.

References

[1] J.Chanard, S. Lavaud, C. Randoux, P. Rieu, Nephrol. Dial. Transplant **18**, 252 (2003).
[2] V. I. Shubayev, R. Brånemark, J. Steinauer, R. R Myers, J. Rehabil. Res. Dev. **41(6A)**, 757 (2004).
[3] J. M. Curran, J.A. Gallagher, J.A. Hunt, Biomaterials **26**, 5313 (2005).
[4] M. J. Allen, N. Rushton, Promega Notes Magazine **45**, 7 (1994).
[5] L. Hartwell, The Scientist **19(18)**, 18 (2005).
[6] N. Johnston, The Scientist **19(13)**, 24 (2005).
[7] V. Henri, Lois générale de l'action de diastases, Hermann, Paris (1903).
[8] L. Michaelis, M. Menten, Biochem Z. **49**, 333 (1913).
[9] D. Voet, J.G. Voet, Biochemistry, second ed., John Wiley and Sons, Inc., New York (1995)
[10] K. J. Laidler, Can. J. Chem. **33**, 1614 (1955).
[11] B. Hayes, American Scientist **93**, 104 (2005).
[12] S. Schnell, C. Mendoza, J. Theor. Biol. **187**, 207 (1997).
[13] S. Schnell, C. Mendoza, Acta Biotheoretica **49**, 109 (2001).
[14] A. Zewail (Editor), The Chemical Bond – Structure and Dynamics, Academic Press, San Diego (1992).
[15] M. V. Putz, A.-M. Lacrămă, V. Ostafe, Proc. VIII-th International Symposium "Young People and Multidisciplinary Research", Timişoara, Welding Publishing House, Association of Multidisciplinary Research of the West Zone of Romania, Timişoara, Romania, 2006, p. 642.
[16] R. A. Copeland, Enzymes, Wiley-VCH, New York (2000).

*Corresponding author: mvputz@cbg.uvt.ro